Available online at www.sciencedirect.com

SciVerse ScienceDirect

Ceramics International 38 (2012) 4707–4713

CERAMICS
INTERNATIONAL

www.elsevier.com/locate/ceramint

Microstructure and mechanical properties of the spark plasma sintered Ta_2C ceramics

Limeng Liu [a,b,*], Han Liu [a], Feng Ye [a], Zhiguo Zhang [b], Yu Zhou [a]

[a] *School of Materials Science and Engineering, Harbin Institute of Technology, Harbin 150001, China*
[b] *Department of Physics, Harbin Institute of Technology, Harbin 150001, China*

Received 12 October 2011; received in revised form 16 February 2012; accepted 16 February 2012
Available online 25 February 2012

Abstract

Single phase hexagonal α-Ta_2C ceramics were synthesized by spark plasma sintering and using TaC and Ta as the starting powders. Effects of sintering temperatures and holding times on the densification process, phase formation, microstructure development, and mechanical properties of the α-Ta_2C ceramics were investigated. Densification occurred in the temperature range of 1520–1675 °C in less than 2.5 min. But completion of the Ta_2C formation took about 40 min at 1500 °C, and 5 min at 1900 °C. The materials sintered at 1500 °C consisted of fine equiaxed grains. The Ta_2C grains grew anisotropic to form an elongated self-toughening microstructure at 1700 °C. At 1900 °C, the neighboring Ta_2C individual crystals coalesced to form large Ta_2C blocks to entrap the residual pores. Although higher flexural strength and fracture toughness were reached at 1700 °C, the unstable microstructures of the Ta_2C materials indicated limited applications at high temperatures.

Keywords: A. Sintering; C. Strength; D. Carbide; Microstructure

1. Introduction

The tantalum carbide compounds have melting points in excess of 3800 °C. The melting points are almost the highest among the ultra-high temperature ceramics (UHTCs), namely the carbides, borides, and nitrides of the IVA–VIA transient metals [1–6]. These UHTCs have attracted intense researches for their potential applications in the future hypersonic flight and the scramjet propulsion components.

Three carbides stoichiometry, i.e. the cubic TaC_y, rhombohedral ζ-Ta_4C_{3-x} and hexagonal Ta_2C with different C were identified in the Ta–C phase diagram [4–6]. Compared to the large stack of studies on the processing, microstructure and mechanical properties of the cubic TaC_y and rhombohedral ζ-Ta_4C_{3-x} ceramics, reports on the single phase α- or β-Ta_2C ceramics are very few and some important data are not available [7–9].

Ref. [10] prepared a W–Ta_2C composite having 48.9 vol.% Ta_2C in the phase composition. The composite was fabricated by first reacting a powder mixture of Ta_2O_5, WC, TaC, and phenolic resin at 1450 °C and by subsequent densifying the resultant powder at 1850 °C. The Young's modulus of the Ta_2C phase was estimated by the rule of mixtures to be 530 GPa. Desmaison-Brut et al. [8] prepared a Ta_2C ceramic with a relative density of ~98% by hot isostatic pressing a TaC and Ta powder mixture at 1630 °C under 195 MPa for 2 h. The obtained Ta_2C exhibited a better oxidation resistance than the TaC ceramic due to the formation of a dense TaC_xO_y layer beneath the porous TaO_2 surface [11]. Alexandre et al. [9] reported the mechanical properties of the same HIP-ed Ta_2C ceramic. The flexural strength, fracture toughness, and Knoop micro-hardness were 550 ± 50 MPa, 9.7 ± 0.8 MPa $m^{1/2}$, and 5.6 ± 0.7 GPa, respectively. However, the effects of the sintering process on the microstructures and mechanical properties are not clear.

More recently, a Ta_2C ceramic was synthesized by the self-propagating high temperature synthesis (SHS) technique at 1800 °C. Ta and C were used as the starting powders [12]. No information on the microstructures and the mechanical properties was reported. Although micrographs and mechanical

---

* Corresponding author at: School of Materials Science and Engineering, Harbin Institute of Technology, Harbin 150001, China. Tel.: +86 451 86413921; fax: +86 451 86413921.
E-mail address: liulimeng@hit.edu.cn (L. Liu).

doi:10.1016/j.ceramint.2012.02.055

properties could be found in Ref. [6], the data were obtained from thin Ta_2C layers produced by carburizing a Ta metal [6], a situation made them unsuitable for technical references. Therefore, it is necessary to fabricate Ta_2C ceramics again and investigate the microstructures and the mechanical properties of the Ta_2C ceramics.

In this study, α-Ta_2C ceramics were synthesized by spark plasma sintering (SPS) at 1500–1900 °C. TaC and Ta powders were used as the starting materials. The phase formation, densification, microstructure development and mechanical properties of the α-Ta_2C ceramics were investigated. SPS was used for its higher sintering efficiency due to its capability of high heating and cooling rate (up to ~600 °C/min and ~400 °C/min, respectively). In comparison, heating and cooling rate of ~50 °C/min can be reached in the conventional hot pressing (HP). Densification may also be accelerated in SPS due to the rapid heating and/or the pulsed electric current passing through the SPS die for heating. Various materials can be sintered in less than 30 min by SPS whereas hours would be taken by HP.

2. Experimental procedures

The starting powders were TaC and Ta (Ningxia Orient Tantalum Industry Co. Ltd., China), both having a purity $> 99\%$, and a mean particle size of 1.25 μm and 0.7 μm, respectively. The main impurities in the TaC powder were ~0.3 wt% Nb, 0.1 wt% Fe, 0.20 wt% O, 0.15 wt% free carbon, 0.05 wt% N, and Al, Ca, K, Na, Ti with a total amount < 0.05 wt%.

Sixty grams of TaC and Ta powder in a molar ratio of 1:1 were ball-mixed for 24 h at 400 rpm in a steel cylinder having a diameter of 50 mm. The inner walls of the cylinder were lined by PVC to prevent Fe contamination from wearing. Three hundred grams of ZrO_2 balls with an average diameter of 5 mm were used as the mixing media.

Batches of the mixture, up to 20 g each, were loaded in graphite SPS dies. The dies have a height of 40 mm and an inner, outer diameter of 20 mm and 50 mm, respectively. SPS sinterings were performed at 1300–1900 °C at 200 °C intervals, for 5–60 min under a 40 MPa uniaxial pressure in a vacuum. A Dr. Sinter 1080 SPS equipment (Sumitomo Coal Mining Company Ltd., Tokyo, Japan) was used. After the furnace was evacuated to <6 Pa, the temperature was automatically increased to 700 °C in 4 min and the pressure increased from 5 MPa to 40 MPa. Thereafter, a heating rate of 100 °C/min was used. After holding for 5–60 min at the preset temperatures, the 40 MPa pressure was released and the SPS power was shut down to allow cooling. The samples were designated by referring both the holding temperatures and the holding time. For example, the 1500 °C/40 min material was the one sintered at 1500 °C for 40 min.

The sintering temperature was measured by a pyrometer focusing on the surface of the SPS die. The SPS equipment had a high resolution data acquiring system to record the densification processes of the powder compacts. The gas pressure of the SPS chamber, ram displacement and displacement rate, mechanical pressure, and the sintering temperature [13] were recorded for further analysis. But it should be pointed out that the ram displacement included not only the densifying shrinkage of the powder compact, but also the thermal expansions, and the strains of the powder compact, the SPS spacers and the punches under the mechanical sintering pressure.

Densities and open porosities of the different samples were measured by the Archimedes method. Room temperature water was used as the immersing media. The relative densities of the samples were calculated as the percent ratios of the measured densities to the theoretical for Ta_2C (15.1 g/cm^3, JCPDS 65-0306). Incompletion of the $TaC + Ta \rightarrow Ta_2C$ reaction would make the theoretical densities of the resultant materials difficult to determine. In this case, 15.1 g/cm^3 was also used as the theoretical. Although this would bring larger test errors, rough comparison should be admissive.

The phase compositions were identified by XRD with a Cu K_α radiation (D/max-γB, Rigaku Rotaflex, Japan). Both polished and fracture surfaces were observed by a FEI-SEM (Nova Nano SEM 50, The Netherlands) with an attached energy dispersive X-ray spectroscope (EDXS). The grain sizes were measured by using an Image-Pro Plus software compact (Media Cybernetics Inc., Silver Spring, MD). The Vickers hardness was tested under a 49 N load for a dwell time of 15 s. The fracture toughness was calculated according to the lengths of the cracks appeared at the corners of the Vickers indentations. For the fracture toughness calculation, the equation proposed by Anstis [14] was applied. Flexure strength was tested by the three-point bending method on an Instron frame (Instron-5566, Instron Corporation, USA). The dimensions of the three-point bending samples were 4.0 mm × 1.5 mm × 18.0 mm, with a 15.0 mm span and 1.5 mm height. The fracture direction was normal to the SPS pressing direction. Young's modulus was calculated by the stress–strain curves recorded by a gauge attached to the tensile surfaces of the bending samples. Three specimens were tested for each condition.

3. Results and discussion

3.1. Densification

3.1.1. The ram displacement

The densification process of the TaC and Ta powder mixture was recorded by the SPS system. The ram displacement, temperature and the gas pressure in the chamber were shown in Fig. 1. Six distinct stages were observed and were marked by I–VI in the ram displacement curve. Although both the strains and the thermal expansions of the powder-SPS die set-up were included in the ram displacement, the ram travel in stage I obviously reflected the enhanced powder packing corresponding to the uniaxial pressure increase from the initial 5 MPa to the final 40 MPa. In stage II the temperature was heated from 700 °C to 1520 °C at 100 °C/min. No shrinkage of the powder compact was observed in this temperature range. The thermal expansions of the SPS die set-up produced the negative slope, indicating no sintering of the powder compact in stage II.

Densifying predominantly occurred in stage III which corresponded to a temperature narrow range of 1520–1675 °C

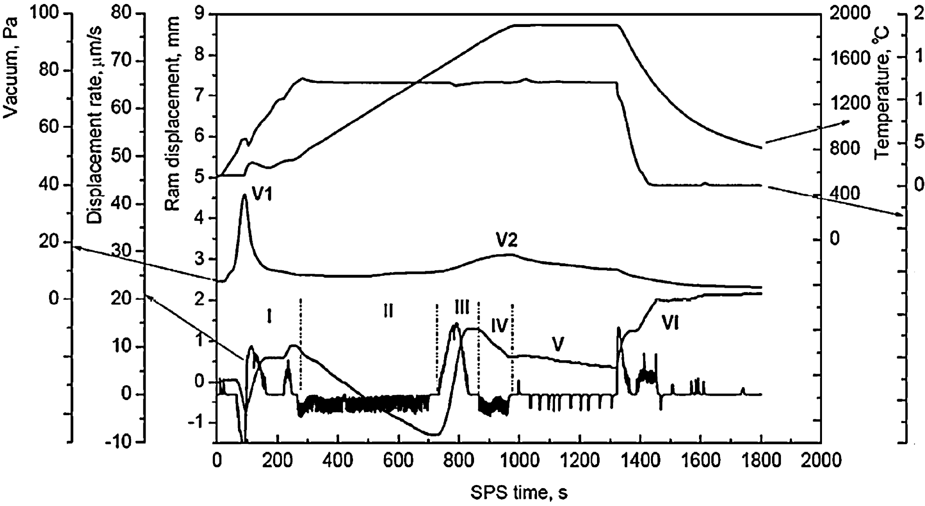

Fig. 1. The SPS ram displacement as a function of the SPS temperature, showing the densification process of the Ta$_2$C composition from the TaC and Ta powder mixture.

and a very short time of ~2.5 min for fixed heating rate. The ram displacement indicated densification completion at 1675 °C. Holding at a higher temperature such as 1700 °C and 1900 °C, or prolonging the sintering time could contribute only a marginal few percents to the final densities.

After densification completion, in the stage IV, expansion of the die set-up produced another negative slope in the displacement curve up to 1900 °C. The next stage V and stage VI were the isothermal holding at the preset 1900 °C and the cooling after sintering, respectively. The graphite spacers isolating the water-cooled SPS rams from the hot SPS punches underwent a heating up by slow thermal conduction. The consequent thermal expansion catch-up of the SPS spacers explained the slight negative slope in stage V. After holding, the 40 MPa sintering pressure was released within 1 min and the SPS power was shut off to allow cooling, hence the ram displacement in stage VI. Finally, the total 2.17 mm ram displacement estimated a relative density of >97%.

3.1.2. Change of the gas pressure in the SPS chamber

A noticeable gas pressure change in the SPS chamber was recorded in Fig. 1, accompanying the densification of the powder mixture. The gas pressure increased from the initial 6 Pa to the maximum 38 Pa at around 700 °C. This maximum gas release was attributed to the de-absorption of the moistures and/or other species such as O_2 and CO_2 in the starting powders. The next max of ~14 Pa in the higher temperature range from ~1550 °C to 1900 °C should come from a gaseous product that was released into the chamber. Here the gaseous product was supposed to include such species as TaO and CO. The chemical components of the vapor were of obvious importance for the densification of the UHTCs, but unfortunately out of the SPS equipment's ability [13]. A gaseous product could indicate the involvement of bad evaporation–condensation in the microstructure formation, because the evaporation mechanism is of high efficiency in coarsening the microstructures, but without densification.

3.1.3. Densities

The densities of the materials were measured by the Archimedes method. The results were listed in Table 1. The results demonstrated that 1500 °C set a temperature limit for sufficient sintering, in agreement with the densification curves shown in Fig. 1. Table 1 shows the 1300 °C/5 min material had a low relative density of 78.3% with a high amount of open pores up to 17.3%. Prolonging the holding time at 1300 °C seemed ineffective in increasing the density. When the holding time was increased from 5 min to 60 min at this temperature, the relative density was only increased by 1.1%.

Sintering at 1500 °C, though this was lower than the densification initiation temperature (1520 °C) in Fig. 1 could

Table 1
Densification, phase compositions and mechanical properties of the Ta$_2$C materials.

SPS condition	Density (g/cm^3)	Relative density (%)	Open porosity (%)	Phase compositions	Vickers hardness (GPa)	Youngs modulus (GPa)	Flexure strength (MPa)	Fracture toughness (MPa m$^{1/2}$)
1300 °C/5 min	11.77	78.34	17.31	Ta$_2$C, Ta, TaC	6.3 ± 0.5	257 ± 26	199 ± 35	1.6 ± 0.2
1300 °C/60 min	12.05	80.15	16.03	Ta$_2$C, Ta, TaC	6.8 ± 0.5	296 ± 23	216 ± 33	1.9 ± 0.2
1500 °C/5 min	13.94	92.72	2.16	Ta$_2$C, Ta, TaC	9.4 ± 0.7	381 ± 19	294 ± 31	3.1 ± 0.4
1500 °C/20 min	14.21	94.57	0.94	Ta$_2$C, trace Ta, TaC	10.3 ± 0.9	403 ± 12	335 ± 29	3.5 ± 0.3
1500 °C/60 min	14.42	95.82	0.31	Ta$_2$C	11.7 ± 0.8	489 ± 11	461 ± 55	4.8 ± 0.7
1700 °C/5 min	14.32	95.23	0.10	Ta$_2$C, trace Ta, TaC	11.4 ± 0.7	481 ± 11	517 ± 49	5.6 ± 0.8
1700 °C/20 min	14.43	95.90	0	Ta$_2$C	11.6 ± 0.8	484 ± 12	548 ± 52	6.0 ± 0.6
1 900 °C/5 min	14.66	97.51	0	Ta$_2$C	11.8 ± 0.9	493 ± 11	507 ± 45	6.4 ± 0.7

significantly increase the relative density. The theoretical density of 1500 °C/5 min material reached 92.7% and the open porosity was reduced to 2.2%. Prolonging the holding to 20 min further reduced the open porosity to the 0.94% level, with a higher relative density of 94.5%. However, 60 min was needed to achieve pore closure and final densities > 95% (Table 1).

Compared to the materials sintered at lower temperatures, the 1700 °C/20 min and 1900 °C/5 min materials had a better relative density of 95.8% and 97.5%, respectively. This evidenced the significant effect of the sintering temperatures on the densification of the Ta_2C ceramics. However, the density measurements indicated that extending the holding time only increased the densities marginally after completion of the pore closure at 1500 °C and 1700 °C. Refs. [8,9] reported a relative density up to ~98% for a Ta_2C ceramic after HIP-ing at 1630 °C under 195 MPa for 2 h. SPS at 1500–1900 °C for 5–60 min under 40 MPa could reach the same density level. But fully dense Ta_2C ceramics could not be obtained.

3.2. Phase formation

The phase formation of the targeted Ta_2C from the TaC and Ta starting powders was investigated by the XRD analysis. The XRD analysis results were listed in Table 1. Selected XRD patterns of the 1300–1900 °C/5 min materials were shown in Fig. 2. The results showed phase composition was dominated by α-Ta_2C after sintering at 1300 °C for 5 min. Small amounts of TaC and Ta were detected in the 1300 °C, the 1500 °C/5–20 min and the 1700 °C/5 min materials, indicating incompletion of the $TaC + Ta \rightarrow Ta_2C$ reaction. When the holding time was prolonged to 40 min and 20 min at 1500 °C and 1700 °C, respectively, the residual TaC and Ta were significantly reduced to produce an almost single phase Ta_2C ceramics.

The phase evolution results suggested that higher temperature was more effective than prolonging the sintering time in promoting the $TaC + Ta \rightarrow Ta_2C$ reaction. The 1900 °C/5 min material exhibited a single phase Ta_2C ceramic.

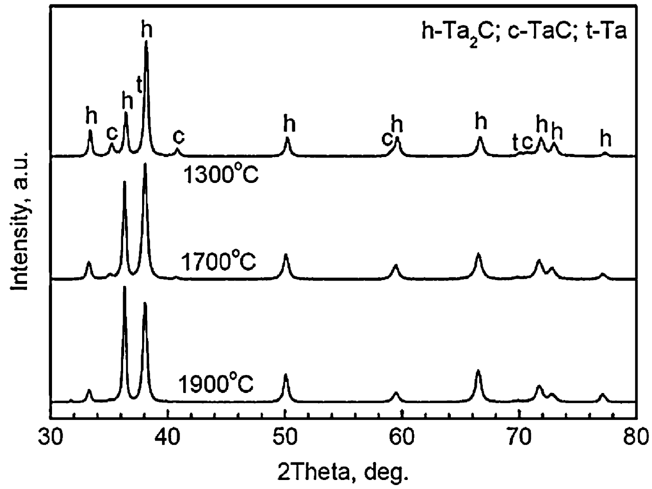

Fig. 2. The typical X-ray diffraction patterns of the Ta_2C materials after sintering for 5 min at the different temperatures.

The Ta–C phase diagram predicts α–β polymorph transformation at about 1530 °C [4–6]. But no β-Ta_2C polymorph was observed in the 1700 °C and the 1900 °C materials, although the sintering temperatures were located in the β phase area in the Ta–C phase diagram [1–3]. The absence of the β-Ta_2C may be due to the slower transformation kinetics for the relatively low sintering temperatures. Literature reported substitution of β- for α-Ta_2C in a Ta/C diffusion couple after carburization at 2150 °C for 8.9 h [3].

3.3. Microstructure development

3.3.1. General observation

The typical microstructures of the Ta_2C ceramics were shown in Fig. 3. The dark and the gray phases in the micrographs were the residual pores and the dominant Ta_2C, respectively. Grain orientation was thought to be the reason for the slight contrast difference for the same Ta_2C phase [15] in Fig. 3c and e. A very small content of residual TaC or Ta grains with a bright contrast was observable in the microstructures of the other 1500 °C and 1700 °C materials, in agreement with the XRD analysis results.

The microstructures of the Ta_2C ceramics were more temperature dependent than the holding times. Fig. 3 shows prolonging the holding time from 5 min to 60 min at 1500 °C and from 5 to 20 min at 1700 °C did not change the microstructures significantly, except for a 20–30% diameter growth of the grains.

3.3.2. The residual pores

The 1300 °C materials had large irregular pores in the microstructures (Fig. 3a). This was in consistency with the low densities listed in Table 1. When the SPS temperature was increased to 1500 °C and above, the improvement of the densification was evident by the significant reduction in both pore concentrations and pore sizes. Fig. 3 shows the average diameters of the residual pores decreased from ~2.0 μm in the 1300 °C material to ~0.4 μm in the 1500 °C material. Sintering at 1900 °C caused rapid coalescence of the neighboring Ta_2C grains to intragranularly entrap the residual pores (Fig. 3g). Our previous report [16] and Zhang et al. [15] observed pores being entrapped by the grains in $TaC_{0.7}$ and TaC ceramics, respectively.

3.3.3. The grain sizes

Fig. 3 revealed a significant effect of the sintering temperatures on the sizes of the Ta_2C grains. An average diameter of ~0.6 μm for Ta_2C grain was obtained in the 1300 °C material which was 50% smaller than the particle sizes of the starting powders. The smaller grains could be explained by a fact that the new Ta_2C phase nucleated and grew by consuming both TaC and Ta particles.

Contrast to the 1300 °C materials, the 1500 °C and 1700 °C materials saw significant Ta_2C grain growth. Fig. 3 shows the 1500 °C and 1700 °C material consisted grains with an average diameter of 1.3 μm and 3.7 μm, respectively. Surprising enlargement of the Ta_2C grains was observed at 1900 °C.

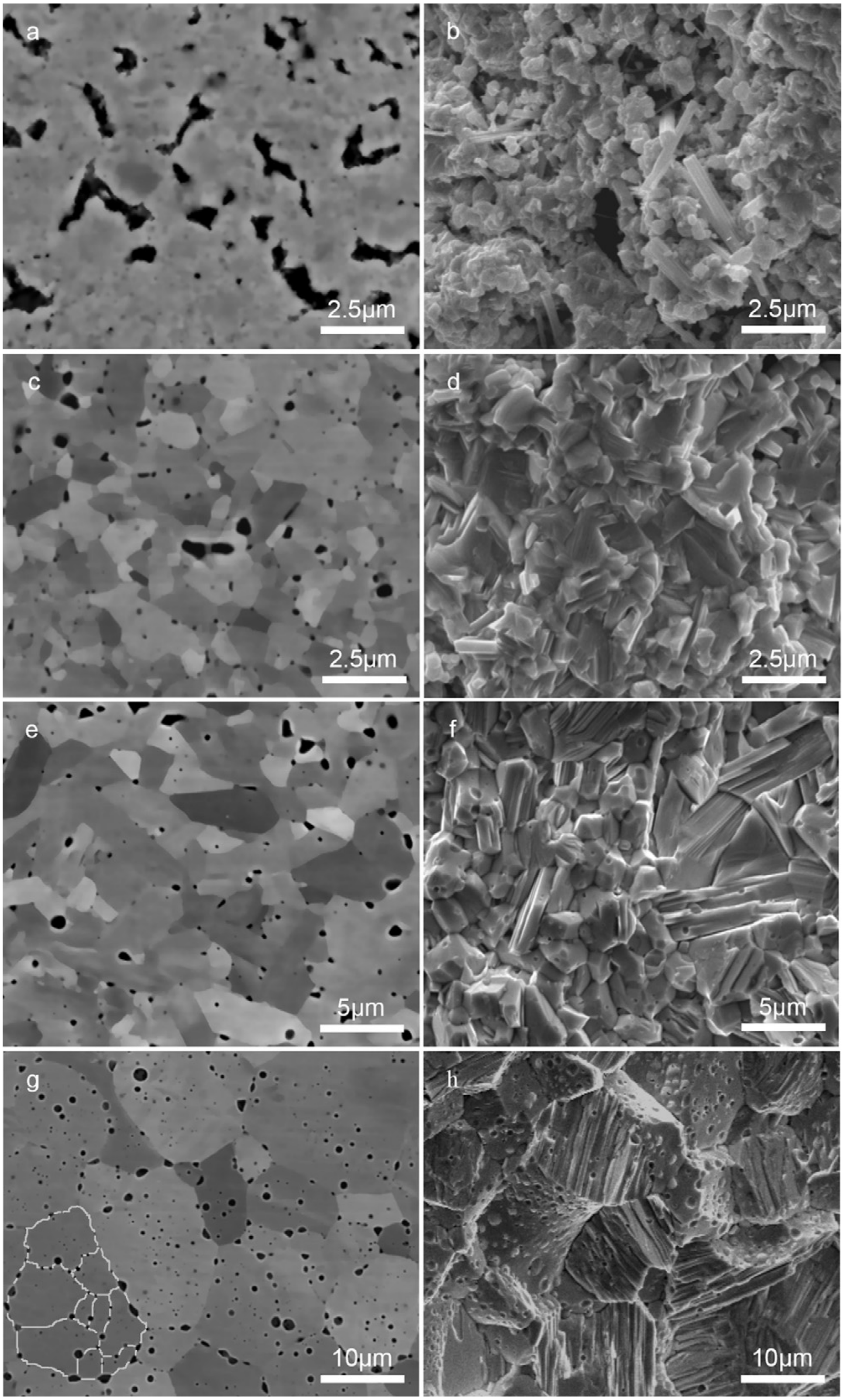

Fig. 3. SEM images of the microstructures (left column) and the fractures (right column) of the Ta_2C materials synthesized by SPS at (a and b) 1300 °C/5 min, (c and d) 1500 °C/60 min, (e and f) 1700 °C/20 min, and (g and h) 1900 °C/5 min. The 1500–1900 °C materials were single phase Ta_2C and had comparable densities. At 1900 °C, the coalescence of the small grains shown by the dot lines formed the significantly enlarged Ta_2C clusters and thus entrapped the residual pores.

Fig. 3g shows in the 1900 °C material rapid coalescence of the neighboring Ta_2C grains formed large clusters with an average diameter of ~17.9 μm. The small Ta_2C single crystals forming a large cluster were still traceable by the entrapped pores. For example, in the bottom left Ta_2C cluster, nine small single crystals could be recognized by the white lines. According to the imaging contrast–orientation relationship proposed by Zhang et al. [15], the single crystals in a large grain should have the same crystal orientation. Therefore the single crystals should have managed to align by an unknown mean in the sintering process to form the large grains. This kind of interesting grain growth behaviors was also observed in α-SiAlON ceramics [17,18] and β-Si_3N_4 ceramics [18], with open debate to the mechanisms.

3.3.4. The grain morphology

Another unique observation of the Ta_2C ceramic microstructures was the dramatic changes in the grain morphologies. Fig. 3c shows the 1500 °C material had an equiaxed microstructure consisting of fine grains with an average diameter of 1.3 μm. Significant elongation at 1700 °C produced an aspect ratio up to ~4.3 of the α-Ta_2C grains in the 1700 °C materials (see Fig. 3e). Such anisotropic grain growth was once reported in Ref. [19,11,20] and was thought beneficial to the fracture toughness. However, at higher temperature of 1900 °C the elongation of the individual grains was completely overwhelmed by the coalescence of the grains to form the equiaxed clusters as shown in Fig. 3g. The reason for the equiaxed grains instead of the elongated to form the large equiaxed Ta_2C clusters was not clear. However mechanical property tests showed the 1900 °C material had a relatively better fracture toughness, maybe due to the fact that the intragranular pores deflect the crack propagations along the former grain boundaries.

3.4. Mechanical properties

The mechanical properties of the Ta_2C ceramics were summarized in Table 1. The differences in densities, the phase compositions and the microstructures should explain the differences in the mechanical properties. In the 1700 °C materials, the presence of the elongated grains in the microstructures should have performed better reinforcement than the smaller equiaxed grains in the 1500 °C materials. The pullout of the plate-like grains and the relatively rougher fracture surface in the fractograph Fig. 3f also indicated more toughening mechanisms. Accordingly, the flexural strength and fracture toughness of the 1700 °C materials were significantly increased in comparison with the 1500 °C materials.

The 1900 °C/5 min material was dominated by intergranular fractures (see Fig. 3). Intragranular fracture was also occasionally observed. The pores distributing along the former boundaries between the individual crystals in the large clusters should have promoted the intragranular fracture and thus deflected the crack tips to give the higher fracture toughness up to 6.4 MPa $m^{1/2}$. However, a higher toughness value of 9.3 MPa $m^{1/2}$ (measured by the single-edge notch beam method) was reported for a HIP Ta_2C ceramic [9,19].

A deleterious effect correlated with the large clusters was demonstrated by the flexural strength. The 1900 °C/5 min material had a flexural strength of 507 MPa, lower than the maximum 548 MPa for the 1700 °C/20 min material. The elongated microstructure in the 1700 °C/20 min material should have perform a better self-reinforcing effect.

The Vickers hardness of 11.6–11.8 GPa for the Ta_2C as listed in Table 1 was similar to Hackett et al. [11], higher than the reported 5.6 GPa for the HIP Ta_2C ceramic [9], but 60% lower than Grossklauss and Bunshah [20] and Teague et al. [10].

For the Young's modules, according to the measured values in Table 1 and the empirical equation [21] of $E = E_0(1 - bP^{2/3})$ (where E and E_0 are the Young's modulus with pores and the ideal modulus without residual pores, P is the porosity, and b is a constant), the Young's modulus of a fully dense Ta_2C ceramic was estimated to be 525 GPa, approaching the reported value of 530 GPa in Ref. [10].

4. Conclusions

(1) Ta_2C ceramics could be densified by spark plasma sintering at 1300 °C and above, using TaC and Ta as the starting powders. Completion of the Ta_2C phase formation took longer time than the densification process.
(2) At 1900 °C, the Ta_2C grains coalesced to form large Ta_2C clusters and entrapped the residual pores, hence prevention of further densification.
(3) The Ta_2C ceramics sintered at 1700 °C exhibited an elongated microstructure to show good combination of flexure strength and fracture toughness.
(4) The microstructures of the Ta_2C ceramics were strongly affected by temperatures. The unstable microstructure with the temperatures should put a limit to the high temperature application of this Ta_2C ceramic.

Acknowledgments

Financial supports from the China Postdoctoral Science Foundation under Grant No. 20090450957 and the Fundamental Research Funds for the Central Universities under Grant No. HIT. NSRIF 2010111 are acknowledged.

References

[1] B. Kim, K. Woo, J. Doh, J. Yoon, I. Shon, Mechanical properties and rapid consolidation of binderless nanostructured tantalum carbide, Ceram. Int. 35 (2009) 3395–3400.
[2] L. Li, Y. Wang, L. Cheng, L. Zhang, Preparation and properties of 2D C/SiC–ZrB_2–TaC composites, Ceram. Int. 37 (2011) 891–896.
[3] J. Chen, Y. Wang, L. Cheng, L. Zhang, Thermal diffusivity of three-dimensional needled C/SiC–TaC composites, Ceram. Int. 37 (2011) 3095–3099.
[4] E.K. Storms, Special report to the phase equilibria program, in: A.E. McHale (Ed.), Phase Equilibria Diagrams, vol. X, American Ceramic Society, Westerville, OH, 1994, pp. 265–266.

[5] A.I. Gusev, A.S. Kurlov, V.N. Lipatnikov, Atomic and vacancy ordering in carbide ζ-Ta_4C_{3-x} ($0.28 \leq x \leq 0.40$) and phase equilibria in the Ta–C system, Solid State Chem. 180 (2007) 3234–3246.

[6] H. Wiesenberger, W. Lengauer, P. Ettmayer, Reactive diffusion and phase equilibria in the V–C, Nb–C, Ta–C and Ta–N systems, Acta Mater. 46 (1998) 651–666.

[7] C.L. Yeh, E.W. Liu, Combustion synthesis of tantalum carbides TaC and Ta_2C, J. Alloys Compd. 415 (2006) 66–72.

[8] M. Desmaison-Brut, N. Alexandre, J. Desmaison, Comparison of the oxidation behaviour of two dense hot isostatically pressed tantalum carbide (TaC and Ta_2C) materials, J. Eur. Ceram. Soc. 17 (1997) 1325–1334.

[9] N. Alexandre, M. Desmaison, F. Valin, M. Boncoeur, Solid state reaction between tantalum (Ta) and tantalum carbide (TaC) powders during HIPing, Key Eng. Mater. 132–136 (1997) 868–871.

[10] M.C. Teague, G.E. Hilmas, W.G. Fahrenholtz, Mechanical properties of reactively processed W/Ta_2C-based composites, J. Eur. Ceram. Soc. 30 (2010) 2197–2201.

[11] K. Hackett, S. Verhoef, R.A. Cutler, D.K. Shetty, Phase constitution and mechanical properties of carbides in the Ta–C system, J. Am. Ceram. Soc. 92 (2009) 2404–2407.

[12] A.L. Bowman, T.C. Wallace, J.L. Yamell, R.G. Wenzel, E.K. Storms, The crystal structures of V_2C and Ta_2C, Acta Crystallogr. 19 (1965) 6–9.

[13] L. Liu, F. Ye, X. He, Y. Zhou, Densification process of TaC/TaB_2 composite in spark plasma sintering, Mater. Chem. Phys. 126 (2011) 459–462.

[14] G.R. Anstis, P. Chantikul, B.R. Lawn, D.B. Marshall, A critical evaluation of indentation techniques for measuring fracture toughness. I. Direct crack measurements, J. Am. Ceram. Soc. 64 (1981) 533–538.

[15] X. Zhang, G.E. Hilmas, W.G. Fahrenholtz, Hot pressing of tantalum carbide with and without sintering additives, J. Am. Ceram. Soc. 90 (2007) 393–401.

[16] L. Liu, F. Ye, Y. Zhou, Z. Zhang, Microstructure and mechanical properties of spark plasma sintered $TaC_{0.7}$ ceramics, J. Am. Ceram. Soc. 93 (2010) 2945–2947.

[17] C. Zhang, K. Komeya, J. Tatami, T. Meguro, Inhomogeneous grain growth and elongation of Dy-α-sialon ceramics at temperatures above 1800 °C, J. Eur. Ceram. Soc. 20 (2000) 939–944.

[18] L. Liu, Microstructure control and mechanical properties of the silicon nitride based ceramics, Dissertation for Doctoral Degree in Engineering, Harbin Institute of Technology, 2007.

[19] N. Alexandre, M. Desmaison, F. Valin, Synthesis of high toughness tantalum carbide Ta_2C by HIP-reaction sintering, in: Hot Isostatic Pressing 93, Proceedings of the International Conference on Hot Isostatic Pressing, 1994, pp. 443–450.

[20] W. Grossklauss, R.F. Bunshah, Synthesis and morphology of various carbides in the tantalum–carbon system, J. Vac. Sci. Technol. 12 (1975) 811–814.

[21] E.A. Dean, J.A. Lopez, Empirical dependence of elastic moduli on porosity for ceramic materials, J. Am. Ceram. Soc. 66 (1983) 366–370.